Journal of Power Sources 192 (2009) 599–605

Contents lists available at ScienceDirect

Journal of Power Sources

journal homepage: www.elsevier.com/locate/jpowsour

Lithium insertion in graphite from ternary ionic liquid-lithium salt electrolytes I. Electrochemical characterization of the electrolytes

Giovanni B. Appetecchi[a,*], Maria Montanino[a], Andrea Balducci[b], Simon F. Lux[b], Martin Winterb, Stefano Passerini[a,b,*]

[a] Agency for the New Technologies, Energy and the Environment (ENEA), TER Department, Via Anguillarese 301, Rome 00123, Italy
[b] Westfälische Wilhelm Universität, Institute of Physical Chemistry, Corrensstr. 28/30, D48149 Münster, Germany

ARTICLE INFO

Article history:
Received 6 October 2008
Received in revised form
28 November 2008
Accepted 20 December 2008
Available online 30 December 2008

Keywords:
N-alkyl-*N*-methylpyrrolidinium
bis(trifluoromethansulfonyl)imide
Ionic liquid
Synthesis
Ionic conductivity
Electrochemical stability

ABSTRACT

In this paper we report the results of chemical-physical investigation performed on ternary room temperature ionic liquid–lithium salt mixtures as electrolytes for lithium-ion battery systems. The ternary electrolytes were made by mixing *N*-methyl-*N*-propyl pyrrolidinium bis(fluorosulfonyl) imide ($PYR_{13}FSI$) and *N*-butyl-*N*-methylpyrrolidinium bis(trifluoromethanesulfonyl) imide ($PYR_{14}TFSI$) ionic liquids with lithium hexafluorophosphate ($LiPF_6$) or lithium bis(trifluoromethanesulfonyl)imide (LiTFSI). The mixtures were developed based on preliminary results on the cyclability of graphite electrodes in the IL-LiX binary electrolytes. The results clearly show the beneficial synergic effect of the two ionic liquids on the electrochemical properties of the mixtures.

1. Introduction

Current high power electrochemical energy storage technologies (rechargeable Li-ion batteries and carbon or hybrid supercapacitors) rely on small amount of electrolytes based on organic, volatile and flammable solvents, which represent major safety problems when applied to many novel applications. In fact, the very small amount of electrolyte present in these devices (necessary for the high power requirement) combined with its low heat capacity makes possible very localized heating to develop in the thermal runaway of the entire device. This, rather than the electrical performance, represents the main drawback presently holding the lithium-ion technology from a wide deployment in hybrid electric vehicles. In order to make high power electrochemical energy storage devices safer and to improve their performance, electrolytes are required that possess the beneficial properties of ILs (absence of volatility, extremely low flammability, high thermal stability and high heat capacity). Ionic liquids (ILs) represent a very interesting new class of room temperature fluids. Their beneficial properties have attracted a large attention for the use of ILs as "green" solvents for chemical reactions, bi-phasic catalysis, chemical synthesis, separations [1–5]. More recently, ILs have been largely investigated as electrolytes (or electrolyte components) for electrochemical devices including rechargeable lithium batteries, fuel cells, double-layer capacitors, hybrid supercapacitors, photoelectrochemical cells, and electrodeposition of electropositive metals [6–16] due to their hydrophobicity, high ionic conductivity and electrochemical stability. In previous papers, [14–16] we successfully demonstrated that addition of ILs as *N*-alkyl-*N*-methylpyrrolidinium bis (trifluoromethanesulfonyl)imides, $PYR_{1A}TFSI$ (A = *n*-propyl or *n*-butyl), to PEO-based membranes enhances the ionic conductivity above 10^{-4} S cm^{-1} at room temperature [16]. PEO-LiX-IL electrolyte systems were tested at low and medium temperatures in dry, all-solid-state, Li/V_2O_5 and Li/$LiFePO_4$ polymer batteries that delivered large capacities with high reversibility and very good cycling performance. We also showed that $PYR_{13}TFSI$ (and its mixtures with LiTFSI) could be incorporated in fluorinated polymer matrices (PTFE and PVdF), which are commonly used as electrolyte membranes (and electrode binders) in lithium and lithium-ion batteries [17]. The resulting solid polymer electrolytes showed good electrochemical performance.

The reversible lithium intercalation into graphite electrode in ionic liquid-based electrolytes, e.g., EMIFSI-LiTFSI, was demonstrated by Ishikawa and co-workers [18]. In this and in a following

* Corresponding author.
E-mail addresses: gianni.appetecchi@casaccia.enea.it (G.B. Appetecchi), stefano.passerini@uni-muenster.de (S. Passerini).

0378-7753/$ – see front matter © 2009 Elsevier B.V. All rights reserved.
doi:10.1016/j.jpowsour.2008.12.095

manuscript we report the results of our investigations for the use of $PYR_{13}FSI$-$PYR_{14}TFSI$-LiTFSI and $PYR_{13}FSI$-$PYR_{14}TFSI$-$LiPF_6$ ternary mixtures as electrolytes for lithium-ion battery systems. The rationale behind the mixing of the two ILs relied on the possibility of combining their different properties with a synergic effect. $PYR_{14}TFSI$ and its mixtures with lithium salts were found to have good room temperature ionic conductivities (> 1 mS cm^{-1}) and overall stability windows exceeding 5.5 V with the cathodic stability limit exceeding the lithium plating/stripping potential [19]. *N*-methyl-*N*-propyl pyrrolidinium bis(fluorosulfonyl)imide, $PYR_{13}FSI$, has shown a lower viscosity because of the reduced steric hindrance of the $(PYR_{13})^+$ cation and, especially, the $(FSI)^-$ anion. In addition, $PYR_{13}FSI$ exhibits a lower melting point thus resulting in its high conductivity values (1.8 mS cm^{-1}) also at low temperatures (−5 °C) [20] In addition, the electrolyte formed by dissolving LiTFSI in $PYR_{13}FSI$ has been reported able to allow reversible lithium insertion/deinsertion in graphite electrodes. Nevertheless, this latter IL ($PYR_{13}FSI$) shows a lower electrochemical stability window than $PYR_{14}TFSI$ and, also important, a much higher cost due to the more difficult purification of the FSI^- anion.

In order to verify if the favorable properties of the two ILs could be combined, blends of $PYR_{13}FSI$ and $PYR_{14}TFSI$ ionic liquids were prepared. The ternary $PYR_{13}FSI$/$PYR_{14}TFSI$/LiX mixtures were obtained by dissolving a suitable lithium salt in the binary $PYR_{13}FSI$-$PYR_{14}TFSI$ blends. The lithium salt $LiPF_6$ and LiTFSI where selected for two different reasons: $LiPF_6$ is the most common lithium salt employed in lithium-ion batteries [21] because it offers good electrolyte conductivities, [22,23] good film-forming ability on carbonaceous anodes [23] and, finally, stabilizes the cathodic (aluminum) current collector toward oxidation [24]. On the other hand, LiTFSI was selected for comparison purposes to investigate the effect of PF_6^- anion ($TFSI^-$ anion is already present in the system).

In this paper we report the electrochemical (ionic conductivity and electrochemical stability window) properties of the ternary $PYR_{13}FSI$/$PYR_{14}TFSI$/$LiPF_6$ and $PYR_{13}FSI$/$PYR_{14}TFSI$/LiTFSI mixtures. The performance of these mixtures as electrolytes for lithium intercalation in graphite will be reported in a following manuscript.

2. Experimental

2.1. Synthesis of ionic liquids

The $PYR_{14}TFSI$ and $PYR_{13}FSI$ room temperature ionic liquids were synthesized through a novel procedure developed at ENEA and described in details in previous papers [14,25]. The chemicals *N*-methylpyrrolidine (97 wt. %), 1-bromopropane (99 wt.%), 1-bromobutane (99 wt.%), ethyl acetate (ACS grade >99.5 wt. %), activated carbon (Darco-G60) and alumina (acidic, Brockmann I) were purchased by Aldrich and used as received. LiTFSI (99.9 wt.%, 3 M battery grade) and LiFSI, lithium bis(fluorosulfonyl)imide (DAICHI KOGYO SEIYAKU Co., LTD, 99.9 wt.%, battery grade) was used as received. Deionized H_2O was obtained with a Millipore ion-exchange resin deionizer. The precursors ($PYR_{13}Br$ and $PYR_{14}Br$) were synthesized by reacting *N*-methylpyrrolidine (PYR_1) with the appropriate bromopropane or bromobutane in presence of ethyl acetate. The ionic liquids were synthesized by reacting aqueous solutions of $PYR_{13}Br$ (or $PYR_{14}Br$) and LiFSI (or LiTFSI). The reaction led to the formation of the hydrophobic $PYR_{13}FSI$ (or $PYR_{14}TFSI$) and hydrophilic LiBr.

The water content in the ionic liquids was measured using the standard Karl Fisher method. The titrations were performed by an automatic Karl Fisher coulometer titrator (Mettler Toledo DL32) in dry-room (R.H. < 0.1%) at 20 °C. The Karl Fisher titrant was a one-component (Hydranal 34836 Coulomat AG) reagent provided from Aldrich.

Table 1
Mole composition of $(x)PYR_{13}FSI/(1-x)PYR_{14}TFSI$/(0.3 M)LiTFSI and $(x)PYR_{13}FSI/(1-x)PYR_{14}TFSI$/(0.3 M)$LiPF_6$ ternary mixtures.

PYR13FSI		PYR14TFSI	
Mole fraction	Weight fraction	Mole fraction	Weight fraction
0	0	1.00	1.00
0.07	0.05	0.93	0.95
0.13	0.10	0.87	0.90
0.25	0.20	0.75	0.80
0.37	0.30	0.63	0.70
0.48	0.40	0.52	0.60
0.58	0.50	0.42	0.50
1.00	1.00	0	0

The parameters x and $(1-x)$ are the mole fractions of $PYR_{13}FSI$ and $PYR_{14}TFSI$, respectively. The weight fractions of $PYR_{13}FSI$ and $PYR_{14}TFSI$ are reported for comparison purpose. The lithium salt (i.e., LiTFSI and $LiPF_6$) concentration was fixed to 0.3 molar.

2.2. Preparation of ternary mixtures

The $(x)PYR_{13}FSI/(1-x)PYR_{14}TFSI/LiPF_6$ (set 1) and $(x)PYR_{13}FSI/(1-x)$ $PYR_{14}TFSI$/LiTFSI (set 2) mixtures were prepared by blending the $PYR_{13}FSI$ and $PYR_{14}TFSI$ ionic liquids in the appropriate proportions. The mole fraction, x, was ranged from 0 through 1. Then, $LiPF_6$ (Merck, battery grade, used as received) and LiTFSI (previously dried under vacuum at 120 °C for 18 h) were dissolved in the $PYR_{13}FSI$/$PYR_{14}TFSI$ blends to obtain a lithium salt mole concentration equal to 0.3 molar. Such a salt concentration was fixed on the basis of preliminary cycling test results obtained on carbonaceous anodes. Table 1 reports the mole composition of the $PYR_{13}FSI$-$PYR_{14}TFSI$-LiX ternary mixtures.

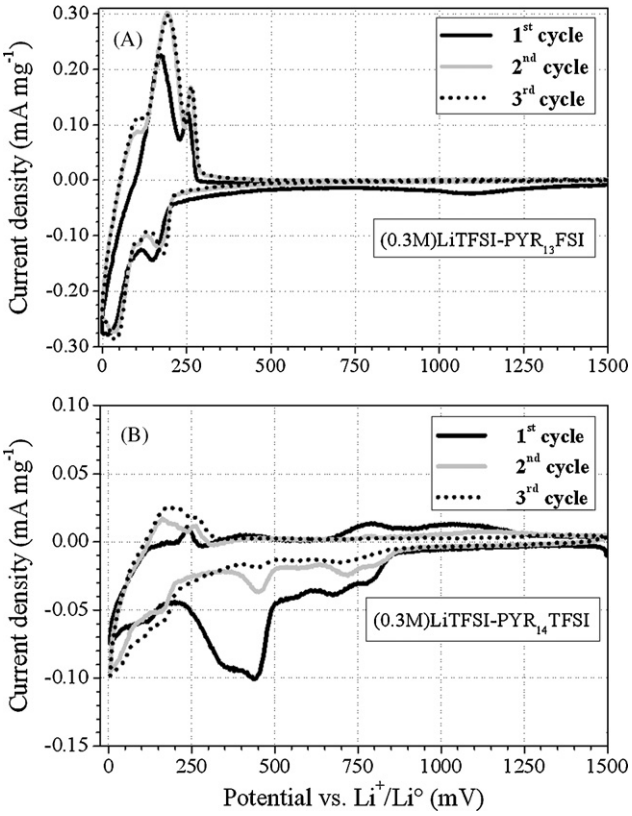

Fig. 1. Initial cyclic voltammetry curves of KS6 graphite composite electrode in (0.3 M)LiTFSI-$PYR_{13}FSI$ (panel A) and (0.3 M)LiTFSI-$PYR_{14}TFSI$ (panel B) electrolytes. Lithium was used for the counter and the reference electrode. Sweep rate: 0.05 mV s^{-1}. *T*: 20 °C.

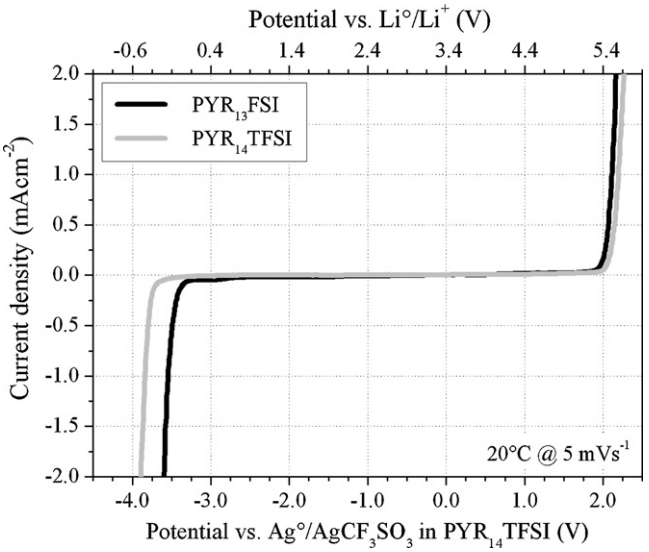

Fig. 2. Linear sweep voltammetries of neat $PYR_{13}FSI$ and $PYR_{14}TFSI$ ionic liquids at 20 °C. Platinum was used for the working and counter electrodes. The reference electrode was a silver wire immersed in a 0.01 M solution of $AgCF_3SO_3$ in $PYR_{14}TFSI$. Scan rate: 5 mV s^{-1}.

2.3. Preparation of graphite electrodes

Graphite electrodes were coated on copper foil by doctor blading a mixture of 90% graphite KS6 (TIMCAL) – 7% Carbon SuperP (TIMCAL) – 3% PVdF binder (Kynar 761, ARKEMA) dispersed in *N*-methylpyrrolidone (NMP, Aldrich). The dried electrodes had an active material mass loading ranging from 0.2 to 0.6 mg cm^{-2}.

2.4. Electrochemical tests

All electrochemical tests were performed in the dry-room. The ionic conductivity of neat $PYR_{13}FSI$ and $PYR_{14}TFSI$ ionic liquids and $(x)PYR_{13}FSI/(1-x)PYR_{14}TFSI/LiX$ mixtures was determined by a conductivity meter AMEL 160. The samples were housed in sealed, glass conductivity cells (AMEL 192/K1) equipped with two porous platinum electrodes (cell constant of 1.00 ± 0.01 cm). The cells were assembled in the dry-room. The conductivity tests were performed in the temperature range from–40 to 100 °C by using a climatic test chamber (Binder GmbH MK53). The entire set-up was controlled by software developed at ENEA.

In order to fully crystallize the materials, the cells were immersed in liquid nitrogen for a few seconds and then transferred in the climatic chamber at −40 °C. After a few minutes of storage at this temperature, the solid but amorphous samples relaxed and turned again liquid. This route was repeated until the ionic liquid and mixture samples remained solid at −40 °C. In previous work it was demonstrated that a not careful crystallization process of the ionic liquid may generate non-equilibrium states of the sample that affect the thermal properties as well as the conductivity results [26] Finally, after a storage period at −40 °C for at least 15 h, the conductivity of the materials was measured in the −40/100 °C temperature range by running a heating scan at 2 °C h^{-1}. For the $LiPF_6$-based mixtures the heating scan was limited to 60 °C in order to minimize the dissociation of $(PF_6)^-$ anion:

$$(PF_6)^- \rightarrow PF_5 + F^- \quad (1)$$

This reaction, promoted by temperature, leads to formation of fluoride anion that in presence of water traces gives hydrofluoric acid (HF) [27,28]. As it is well known, the latter is not welcome in electrochemical devices since irreversible decomposition phenomena may occur (i.e., corrosion of current collector, etc.) [27,28].

The electrochemical stability window of neat $PYR_{13}FSI$ and $PYR_{14}TFSI$ ionic liquids and $(x)PYR_{13}FSI/(1-x)PYR_{14}TFSI/LiX$ mixtures was evaluated by linear sweep voltammetries (LSVs) at 5 mV s^{-1}. A sealed, three-electrode, glass micro-cell, described in details in a previous paper, [29] was used for the LSV tests. The cell was loaded with a small amount of ionic liquid or mixture sample (about 0.5 ml). A glass-sealed, platinum working microelectrode (active area = 0.78 mm^2) and a platinum foil counter electrode (about 0.5 cm^2) were used. The reference electrode was a silver wire immersed in a 0.01 M solution of $AgCF_3SO_3$ in $PYR_{14}TFSI$, separated from the cell compartment with a fine glass frit. This reference electrode, proposed elsewhere, [30–33] was found to be stable for at least 3 weeks. High purity argon (3 ppmv water and 2 ppmv oxygen) was flown over the ionic liquid or mixture sample under investigation for 30 min before the start of the test. The gas flow was continued during the experiment. Separate LSV tests were carried out on each sample to determine the cathodic and anodic electrochemical stability limits. The measurements were performed scanning the cell potential from the open circuit potential (OCP) towards more negative (cathodic limit) or positive (anodic

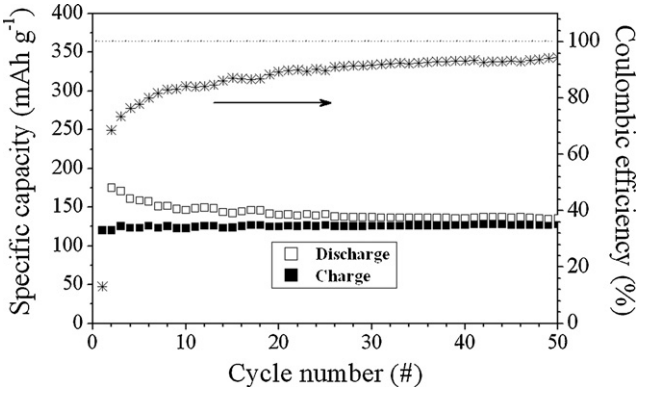

Fig. 3. Cycle performance of KS6 graphite composite electrode in (0.3 M)LiTFSI-$PYR_{13}FSI$ electrolyte. Lithium was used for the counter and the reference electrode. Charge/discharge rate: 1C. *T*: 20 °C.

Table 2
Lithium intercalation/deintercalation capacity in composite graphite electrodes recorded during cyclic voltammetry experiments (Fig. 1A).

Electrolyte	Cycle	Insertion capacity (mA h g^{-1})	Deinsertion capacity (mA h g^{-1})	Reversibility (%)
0.3 M LiTFSI in $PYR_{13}FSI$	1	443.4	128.9	29.1
	2	283.1	219.6	77.6
	3	278.1	232.6	83.6
	Film formation capacity: 108.8 mA h g^{-1} (24.5% of 1st cycle charge capacity)			
0.3 M LiTFSI in $PYR_{14}TFSI$	1	302.4	45.1	14.9
	2	174.5	36.6	21.0
	3	167.3	43.1	25.7
	Film formation capacity: 114.2 mA h g−1 (37.7% of 1st cycle charge capacity)			

The film formation capacity corresponds to the charge consumed above 500 mV during the first intercalation process.

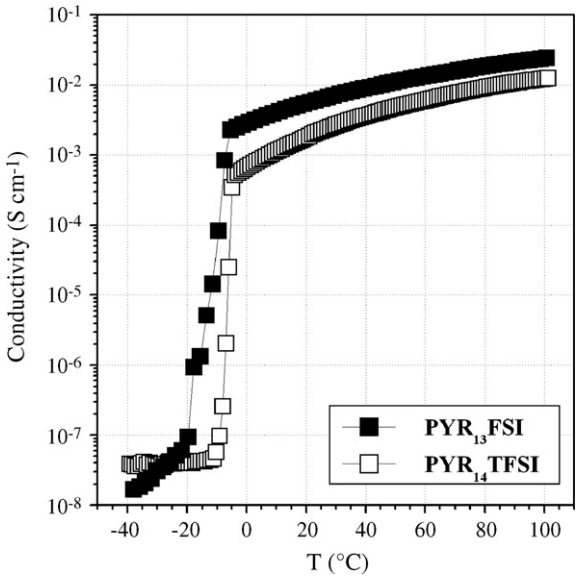

Fig. 4. Ionic conductivity vs. temperature dependence of neat $PYR_{13}FSI$ and $PYR_{14}TFSI$ ionic liquids.

limit) voltages. Clean electrodes and a fresh sample were used for each test. To confirm the results obtained the LSV tests were performed at least twice on different fresh samples of neat $PYR_{13}FSI$ and $PYR_{14}TFSI$ and each x)$PYR_{13}FSI$/$(1-x)$$PYR_{14}TFSI$/LiX mixture. The measurements were performed at 20 °C using an Schlumberger (Solartron) electrochemical interface (model 1287) controlled by a software developed at ENEA.

Sealed Li/graphite (T-shaped) cells were assembled in a dry-box (H_2O and O_2 content < 1 ppm). The cells were made sandwiching a lithium anode (foil), a polypropylene separator (Freudenberg fleeces FS2190) and a composite graphite anode. A lithium metal strip was used as reference electrode. The electrolyte was a 0.3 M solution of LiTFSI dissolved in $PYR_{14}TFSI$ or in $PYR_{13}TFSI$. The cells were investigated by cyclic voltammetry (Adesys CV setup) and galvanostatic charge-discharge cycling tests (Maccor S4000 Battery Tester).

3. Results and discussion

The lithium insertion process in carbonaceous materials from IL-based electrolytes was performed on graphite composite electrodes. Commercial KS6 TIMCAL was selected as the active material because it displays high cristallinity and specific area ($20\,m^2\,g^{-1}$) and, most important, it is very sensitive to the electrolyte properties. This latter characteristic makes it as an appropriate candidate for the investigation of the SEI formation mechanism at the electrode/electrolyte (IL) interface. The SEI growth on graphite electrode in FSI-based electrolyte was previously investigated by Ishikawa and co-workers [34]. We used LiTFSI as lithium salt because the $TFSI^-$ anion was already present in one of the two ionic liquids ($PYR_{14}TFSI$). Fig. 1 illustrates the cyclic voltammograms of KS6-based electrodes in 0.3 M LiTFSI dissolved in $PYR_{13}FSI$ (panel A) and $PYR_{14}TFSI$ (panel B). The *V–I* curves appear to be strongly affected by the ionic liquid used in the electrolyte formulation. In fact, the electrochemical behavior of the graphite electrode in 0.3 M LiTFSI in $PYR_{13}FSI$ corresponds to the well-know lithium staging insertion (each peak corresponds to the formation of a specific stage in lithiated graphite). In the first cathodic sweep, a broad feature, centered at about 1.1 V vs. Li, is observed. In the following cycles no current flow is observed at potential above 0.4 V vs. Li indicating that this irreversible reaction takes place only in the first cathodic cycle. Completely different is the behavior of the graphite electrode in 0.3 M LiTFSI in $PYR_{14}TFSI$. Here, a sequence of peaks is observed between 0.8 V vs. Li and 0.25 V vs. Li most likely correlated with the ionic liquid cation (PYR_{14}^+) insertion in graphite. At lower potentials, the lithium intercalation process takes place. In the following anodic scan several peaks are observed that correspond to the deinsertion of Li^+ and PYR_{14}^+. However, the process is overall strongly irreversible.

The reason of this very different behavior resides, surprisingly, in the enhanced cathodic stability of $PYR_{14}TFSI$ with respect to $PYR_{13}FSI$ (see Fig. 2). In fact, graphite electrodes are not able to reversibly cycle lithium unless they are protected with the lithium-ion conducting SEI layer that avoids solvent molecules or other cations to enter the layered graphite structure. When $PYR_{13}FSI$ was used, the SEI formed as indicated by the appearance of the fully irreversible peak centered at about 1.1 V vs. Li. A similar irreversible peak was not observed with $PYR_{14}TFSI$.

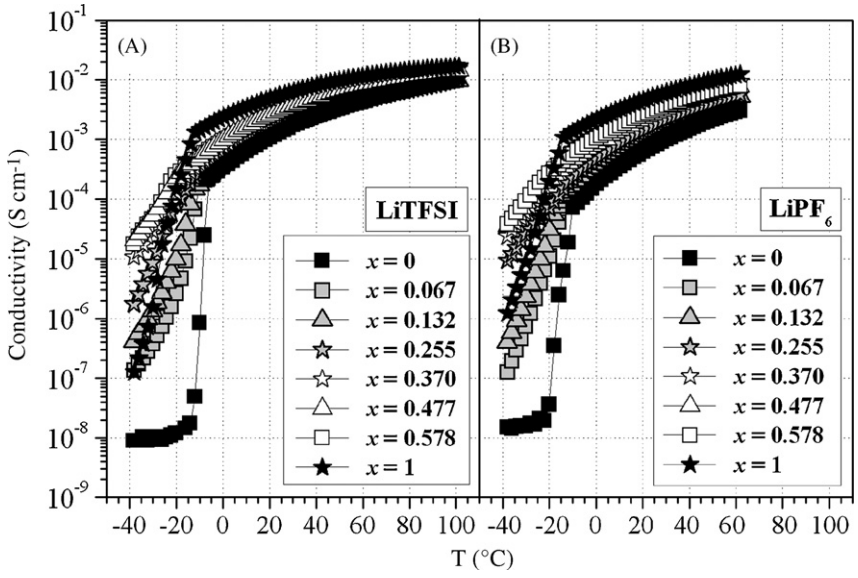

Fig. 5. Ionic conductivity vs. temperature dependence of $(x)PYR_{13}FSI/(1-x)$ $PYR_{14}TFSI$/(0.3 M)LiTFSI (panel A) and $(x)PYR_{13}FSI/(1-x)$ $PYR_{14}TFSI$/(0.3 M)$LiPF_6$ (panel B) ternary mixtures.

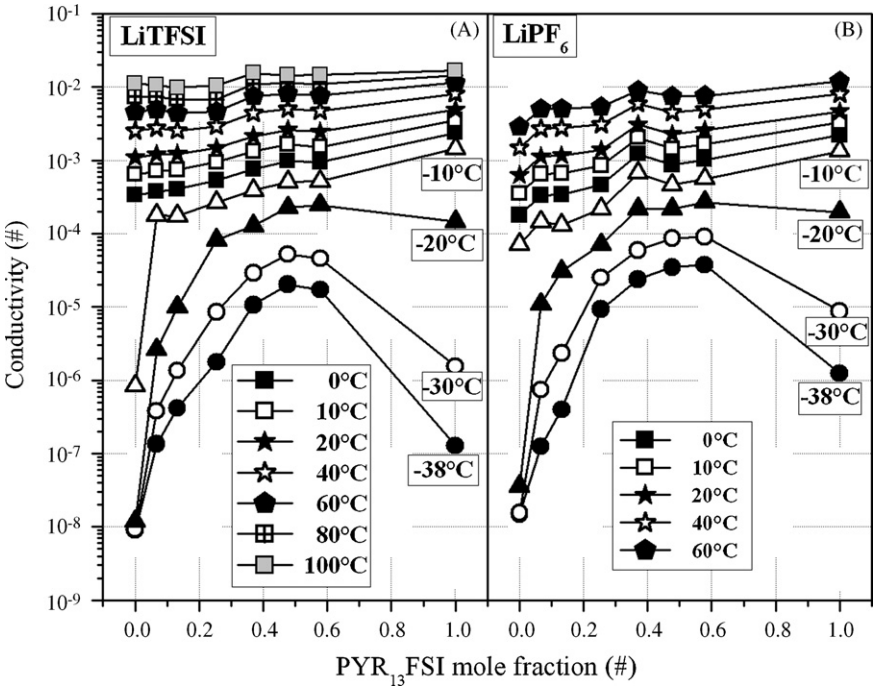

Fig. 6. Ionic conductivity vs. $PYR_{13}FSI$ mole fraction dependence for $(x)PYR_{13}FSI/(1-x)PYR_{14}TFSI$/(0.3 M)LiTFSI (panel A) and $(x)PYR_{13}FSI/(1-x)$ $PYR_{14}TFSI$/(0.3 M)$LiPF_6$ (panel B) ternary mixtures at different temperatures.

The lithium insertion and deinsertion capacities recorded during the CV tests described above are reported in Table 2. As it is easily seen, the $PYR_{13}FSI$-based electrolyte allowed lithium intercalation in graphite, however, the delivered capacity (i.e., the lithium charge released during the anodic scan) was "somehow" limited to about 75% of the typical graphite capacity. The reduction of delivered capacity is even more marked in galvanostatic charge/discharge tests at elevated rate (C rate). In Fig. 3 it is seen that the lithium intercalation in the graphite electrode in 0.3 M LiTFSI in $PYR_{13}FSI$ is very reversible and stable on cycling. However, the overall delivered capacity in the constant current cycling tests was only 140 mA h g^{-1}, i.e., less than 40% of the theoretical capacity. Moreover it was not possible to obtain a constant current cycling measurement with the $PYR_{14}TFSI$ due to the absence of the protecting SEI layer.

In an effort to combine the good electrochemical stability of the $PYR_{14}TFSI$ and the SEI-forming ability and high ionic conductivity (see Fig. 4) of $PYR_{13}FSI$, mixtures of the two ionic liquids were made and used to dissolve two different lithium salts, (LiTFSI and $LiPF_6$ see Table 1 for the detailed composition of the ternary mixtures). Fig. 5 illustrates the ionic conductivity of the mixtures. At a first sight it is seen that the ionic conductivity of the ternary mixtures increases with increasing the fraction of $PYR_{13}FSI$ independent on the salt used. However, a careful observation shows that this trend is true only at temperatures above the melting point of the LiX-$PYR_{13}FSI$ mixture. At lower temperatures, in fact, a few ternary mixtures (LiX-$PYR_{14}TFSI$-$PYR_{13}FSI$) show a higher ionic conductivity than the binary LiX-$PYR_{13}FSI$ mixture. This interesting effect, better observed in Fig. 6, is due to "ionic confusion" present in the mixtures that shifts the crystallization to much lower temperatures. At very low temperatures (−38 °C) the ionic conductivity of the ternary mixtures with the $PYR_{13}FSI$ mole fraction ranging between 0.4 and 0.6 is from two to three orders of magnitude higher than that of the two binary mixtures. This synergic conductivity effect shown by ionic liquid mixtures might have very important technological applications since it certainly facilitates the search for low temperature ionic liquid-based electrolytes.

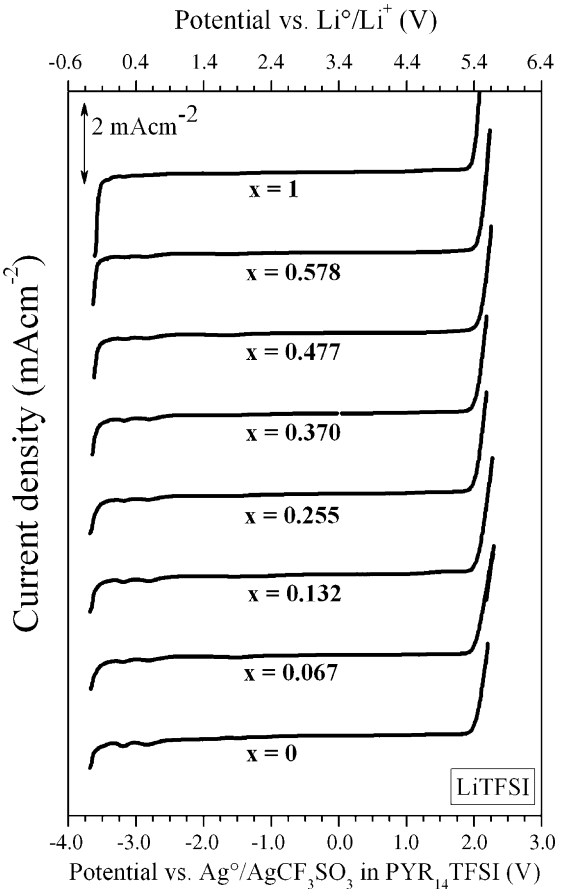

Fig. 7. Linear sweep voltammetries of $(x)PYR_{13}FSI/(1-x)PYR_{14}TFSI$/(0.3 M)LiTFSI ternary mixtures at 20 °C. Platinum was used for the working and counter electrodes. The reference electrode was a silver wire immersed in a 0.01 M solution of $AgCF_3SO_3$ in $PYR_{1n4}TFSI$. Scan rate: 5 mV s^{-1}.

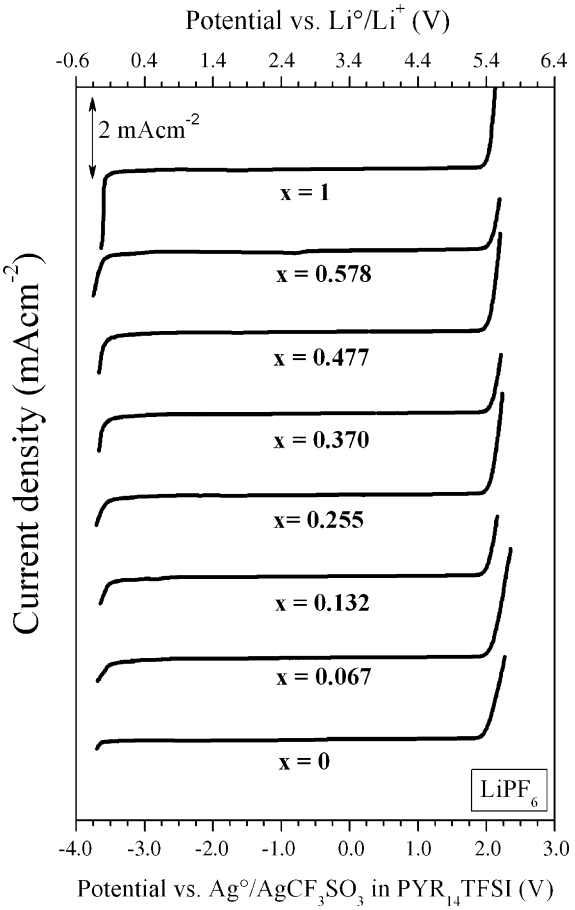

Fig. 8. Linear sweep voltammetries of $(x)PYR_{13}FSI/(1-x)PYR_{14}TFSI/(0.3\,M)LiPF_6$ ternary mixtures at 20 °C. Platinum was used for the working and counter electrodes. The reference electrode was a silver wire immersed in a 0.01 M solution of $AgCF_3SO_3$ in $PYR_{1n4}TFSI$. Scan rate: 5 mV s^{-1}.

Figs. 7 and 8 illustrate the electrochemical stability windows of the ternary mixtures investigated. All mixtures showed ESWs exceeding 5 V with the capability to allow lithium metal plating. The lithium plating current (cathodic limit) strongly enhances with increasing the mole fraction of $PYR_{13}FSI$. This effect is obviously due to the increased ionic conductivity of the electrolytes. The LiTFSI-containing mixtures (Fig. 7) show two small cathodic peaks at about −2.8 and −3.1 V (vs. Ag^0/Ag^+). The origin of these peaks, which are absent in the ESW curves of the $LiPF_6$ ternary mixtures (Fig. 8) and in the ESW curves of the two pure ionic liquids (Fig. 2), is a real puzzle. They can only be related to the LiTFSI salt added in these ternary mixtures. In fact, Li^+ cations and $TFSI^-$ anions are present in all the mixtures but the LiTFSI salt is added only in the series of mixtures showing the two peaks. On the other hand, the intensity of these two peaks clearly increases (see Fig. 7) on increasing the $TFSI^-$ concentration independent on the origin of the $TFSI^-$. The only possible explanation for these experimental evidences is that the LiTFSI salt contains some impurity that acts as a catalyst for the decomposition of the $TFSI^-$ anions. These impurities, however, must be eliminated during the $PYR_{14}TFSI$ synthesis since we did not find any evidence of such peaks in the cathodic stability window of this ionic liquid (see Fig. 2).

LiTFSI has been reported to have a very high thermal stability (decomposition beginning at 360 °C under argon for a 10 °C min^{-1} heating rate) [35] However, we have frequently observed that the commercially available white salt discolored during drying by heating at 180 °C under vacuum for prolonged period of time (at least 12 h). When the salt was then dissolved in anhydrous acetonitrile, the resulting solution had a faint reddish-brown color. This solution filtered through 0.2 μm PTFE filter activated alumina gives a clear, colorless solution and a brownish precipitate on the filter. The white salt, obtained on removal of the acetonitrile by vacuum drying, does not show any discoloration of subsequent drying at 175–185 °C under vacuum. These observations suggest that the LiTFSI salt may contain a small amount (< 0.05 wt%) of an impurity, which is thermally unstable. The identity of this impurity is unknown and the amount of brown precipitate collected on the filter is too low for analysis. However, it is reasonable to assume that the impurities might consist of fractions of the $TFSI^-$ anion, which would also explain the observations made by MacFarlane and colleagues [30] in their study on the cathodic stability on *N*-methyl-*N*-propylpyrrolidinium TFSI. They have, in fact, already reported the existence of the two peaks observed in Fig. 7.

On the other hand, the anodic decomposition limit appears to be very similar for all mixtures as expected considering that the two ionic liquid anions ($TFSI^-$ and FSI^-) (see Fig. 2) and PF_6^- have very similar anodic decomposition limit.

4. Conclusions

In this paper we have reported the results of the chemical–physical investigation performed on ternary room temperature ionic liquid–lithium salt mixtures as electrolytes for lithium-ion battery systems. The ternary electrolytes were made by mixing *N*-methyl-*N*-propyl pyrrolidinium bis(fluorosulfonyl)imide ($PYR_{13}FSI$) and *N*-butyl-*N*-methylpyrrolidinium bis(trifluoromethanesulfonyl)imide ($PYR_{14}TFSI$) ionic liquids with lithium hexafluorophosphate ($LiPF_6$) or lithium bis(trifluoromethanesulfonyl)imide (LiTFSI).

The mixtures, developed based on preliminary results on the cyclability of graphite electrodes in the IL-LiX binary electrolytes, have shown a very wide ESW with the capability of allowing lithium metal plating and stripping.

Finally, the conductivity results clearly indicated a beneficial synergic effect of the two ionic liquids with the ternary mixtures showing higher ionic conductivities than the binary IL-LiX mixtures.

Acknowledgments

The authors wish to thank the financial support of the European Commission within the FP6 STREP Projects ILHYPOS (Contract n° TST4-CT-2005-518307) and ILLIBATT (Contract n° NMP3-CT-2006-033181).

References

[1] P. Wasserscheid, W. Keim, Angew. Chem., Int. Ed. 39 (2000) 3772.
[2] R.D. Rogers, K.R. Seddon Eds., Ionic Liquids-Industrial Application to Green Chemistry; ACS Symposium Series 818; Oxford University Press, 2002.
[3] M.J. Earle, K.R. Seddon, Pure Appl. Chem. 72 (2000) 1391.
[4] J.L. Anderson, T. Ding, D.W. Welton, Armstrong, J. Am. Chem. Soc. 124 (2002) 14247.
[5] J. Dupont, R.F. de Souza, P.A.Z. Suarez, Chem. Rev. 102 (2002) 3667.
[6] A.I. Bhatt, I. May, V.A. Volkovich, M.E. Hetherington, B. Lewin, R.C. Thied, N.J. Ertok, Chem. Soc., Dalton Trans. (2002) 4532.
[7] S. Panozzo, M. Armand, O. Stephan, Appl. Phys. Lett. 80 (2002) 679.
[8] P. Wang, S.M. Zakeeruddin, I. Exnar, M. Gratzel, Chem. Comm. (Cambridge) (2002) 2972.
[9] J. Fuller, A.C. Breda, R.T. Carlin, J. Electroanal. Chem. 29 (1998) 459.
[10] H. Nakagawa, S. Izuchi, K. Kunawa, T. Nukuda, Y. Aihara, J. Electrochem. Soc. 150 (2003) A695.
[11] H. Sakaebe, H. Matsumoto, Electrochem. Commun. 5 (2003) 594.
[12] A. Noda, M.A.B.H. Susan, K. Kudo, S. Mitsushima, K. Hayamizu, M. Watanabe, J. Phys. Chem. B 107 (2003) 4024.
[13] A. Balducci, W.A. Henderson, M. Mastragostino, S. Passerini, P. Simon, F. Soavi, Electrochim. Acta 50 (2005) 2233.
[14] J.-H. Shin, W.A. Henderson, S. Passerini, J. Electrochem. Soc. 152 (2005) A978.
[15] J.-H. Shin, W.A. Henderson, S. Passerini, Electrochem. Sol. St. Lett. 8 (2005) A125.

[16] J.-H. Shin, W.A. Henderson, G.B. Appetecchi, F. Alessandrini, S. Passerini, Electrochim. Acta 50 (2005) 3859.
[17] C. Tizzani, G.B. Appetecchi, M. Carewska, G.-T. Kim, S. Passerini, Aust. J. Chem. 60 (2007) 47.
[18] M. Ishikawa, T. Sugimoto, M. Kikuta, E. Ishiko, M. Kono, J. Power Sources 162 (2006) 658.
[19] G.B. Appetecchi, M. Montanino, D. Zane, M. Carewska, F. Alessandrini, S. Passerini, Electrochim. Acta 54 (2009) 1325.
[20] Q. Zhou, W. Henderson, G.B. Appetecchi, M. Montanino, S. Passerini, J. Phys. Chem. B 112 (2008) 13580.
[21] C.A. Vincent, B. Scrosati, Modern Batteries: An Introduction to Electrochemical Power Sources, 2nd ed., Arnold, London, 1997.
[22] J. Barthel, H.J. Gores, in: J.O. Besenhard (Ed.), Handbook of Battery Materials, Wiley-VCH, Weinheim, 1999.
[23] M. Masayuki, M. Ishikawa, Y. Matsuda, in: M. Wakihara, O. Yamamoto (Eds.), Lithium Ion Batterie, Wiley-VCH, Weinheim, 1998.
[24] S.S. Zhang, T.R. Jow, J. Power Sources 109 (2002) 458–464.
[25] G.B. Appetecchi, S. Scaccia, C. Tizzani, F. Alessandrini, S. Passerini, J. Electrochem. Soc. 153 (2006) A1685.
[26] W.A. Henderson, S. Passerini, Chem. Mater. 16 (2004) 2881.
[27] E. Sloop, J.K. Pugh, S. Wang, J.B. Kerr, K. Kinoshita, Electtrochem, Solid State Lett. 4 (2001) A42.
[28] A.M. Anderson, K. Edstrom, J. Electrochem. Soc. 148 (2001) A1100.
[29] S. Randström, G.B. Appetecchi, C. Lagergren, A. Moreno, S. Passerini, Electrochim. Acta 53 (2007) 1837–1842.
[30] P.C. Howlett, E.I. Izgorodina, M. Forsyth, D.R. MacFarlane, Z. Phys. Chem. 220 (2006) 1483.
[31] Y. Katayama, H. Onodera, M. Yamagata, T. Miura, J. Electrochem. Soc. 151 (2004) A59.
[32] Y. Katayama, K. Sekiguchi, M. Yamagata, T. Miura, J. Electrochem. Soc. 152 (2005) E247.
[33] G.A. Snook, A.S. Best, A.G. Pandolfo, A.F. Hollenkamp, Electrochem. Commun. 8 (2006) 1405.
[34] T. Sugimoto, M. Kikuta, E. Ishiko, M. Kono, M. Ishikawa, J. Power Sources 183 (2008) 436.
[35] L.A. Dominey, V.R. Koch, T.J. Blakley, Electrochim. Acta 37 (1992) 1551.